Characterizing the intestinal chondroitin sulfate glycosaminoglycan sulfation signature in inflammatory bowel disease

Kendra L. Francis
   Seattle Children's Hospital

Hengqi (Betty) Zheng
   Seattle Children's Hospital

David L. Suskind
   Seattle Children's Hospital

Bao Anh Phan
   University of Washington Medicine Diabetes Institute

Mason Nuding
   Seattle Children's Hospital

Alexandra Hudson
   Seattle Children's Hospital

Gregory J. Morton
   University of Washington Medicine Diabetes Institute

Michael W. Schwartz
   University of Washington Medicine Diabetes Institute

Kimberly M. Alonge
   University of Washington Medicine Diabetes Institute

Jarrad M. Scarlett (✉ jarrad.scarlett@seattlechildrens.org)
   Seattle Children's Hospital

Additional Declarations: No competing interests reported.

Abstract

The intestinal extracellular matrix (ECM) helps maintain intestinal homeostasis, and pathologic ECM remodeling is implicated in inflammatory bowel disease (IBD). Chondroitin sulfate and dermatan sulfate glycosaminoglycans (CS/DS-GAGs) are integral components of the ECM, and alterations in CS/DS-GAGs significantly influence its function. However, it is unknown whether changes in CS/DS-GAG composition are linked to IBD. Our aim was to characterize the intestinal ECM CS/DS-GAG composition in active IBD using mass spectrometry to analyze intestinal biopsy samples. We characterized the intestinal CS/DS-GAG composition in 50 pediatric and young adult patients (n = 13 control, n = 37 IBD; age 7–23) and 6 adult patients (n = 6 control, age 24–67). The abundance of isomers associated with matrix stability (CS-A and DS) was significantly decreased in patients with IBD compared to controls, while isomers implicated in inflammation (CS-C and CS-E) were significantly increased. This imbalance of intestinal CS/DS isomers was restored among patients achieving clinical remission. Across the entire cohort, the abundance of pro-stabilizing CS/DS isomers negatively correlated with clinical disease activity scores, whereas both CS-C and CS-E content positively correlated with disease activity scores. Thus, pediatric patients with active IBD exhibited increased pro-inflammatory and decreased pro-stabilizing CS/DS isomer composition, and future studies are needed to determine whether changes in the CS/DS-GAG composition play a pathogenic role in IBD.

INTRODUCTION

Inflammatory bowel disease (IBD) is a chronic inflammatory condition of the gastrointestinal (GI) tract that now affects more than 7 million people worldwide.[1,2] IBD is generally classified into two main subtypes, Crohn's disease (CD) and ulcerative colitis (UC), with a smaller, third subset encompassing individuals with IBD-unclassified. Despite the increasing emergence of new therapeutic options, including state-of-the-art biologic therapies and small molecule inhibitors that target specific components of the immune response,[3,4] IBD continues to prove difficult to control, with many patients requiring multiple medications and surgery.[5–7] Mucosal healing has emerged as a key therapeutic goal in the clinical management of IBD,[3,8] as it is associated with sustained clinical remission (CR), reduced hospitalizations, resection-free survival, and decreased cancer rates.[9–11] However, our ability to achieve this outcome for most patients remains limited by our incomplete understanding of underlying disease mechanisms.

Increasing evidence suggests that the pathogenesis of IBD involves a combination of genetic predisposition, environmental triggers, immune dysregulation, and altered intestinal barrier integrity.[12–14] In light of recent work suggesting that intestinal barrier dysfunction plays an important role in IBD pathogenesis,[15–17] strategies aimed at restoring barrier function may represent a novel strategy to improve disease management and help achieve mucosal healing. Crucial to the integrity of the intestinal barrier is the intestinal extracellular matrix (ECM), a complex, organized network of proteins and glycans that provide physical protection and scaffolding.[18–20] The ECM dynamically regulates the ability of the

intestinal barrier to interact with the surrounding environment and gut microbiome, and is fundamental in cell-to-cell communication via its close connections with integrins and related molecules.[21–23] Specific ECM components, including proteoglycans and their glycosaminoglycan chains, can alter the intestinal microbiota,[24] suppress the expression of pro-inflammatory cytokines,[25,26] and participate in other mucosal inflammatory processes that are a pathologic hallmark of IBD.[18,19,27] Based on these considerations, the ECM has emerged as a potential therapeutic target to promote mucosal healing in IBD.

Chondroitin sulfate (CS) proteoglycans with their protein core and attached CS and dermatan sulfate (DS) glycosaminoglycan (CS/DS-GAG) chains are abundant components of the intestinal ECM (Fig. 1a-b). CS/DS-GAG chains consist of repeating, variably sulfated disaccharide isomers,[28] each of which is identified by a unique sulfation pattern that associates with specific biological functions (Fig. 1c). The relative abundance of the various CS/DS isomers influences the interaction between various cell types and their surrounding environment and has been shown to be altered in certain disease states.[28–30] The mono-sulfated CS-A isomer, which has a sulfate on the 4th carbon (4S) of the N-acetylgalactosamine (GalNAc), is the most abundant isomer and contributes to structural matrix stability.[31–33] Far less abundant is di-sulfated CS-B isomer, known as DS, which is sulfated on the 2nd carbon of the Iduronic acid (IdoA) and 4th carbon of the GalNAc (2S4S) and is implicated in matrix stability and tissue regeneration.[34,35] By comparison, the roles played by the mono-sulfated CS-C isomer, 6th carbon sulfate attachment to GalNAc (6S) and the di-sulfated CS-E isomer, 4th and 6th sulfate attachment to the GalNAc (4S6S), are distinctly different—both are implicated in the inflammatory response and accelerated cell turnover.[28,31,36–39] Lastly, the non-sulfated CS-O (0S) isomer plays a key role in regulating tissue diffusion and permeability.[40]

In addition to the relative abundance of these five CS/DS isomers, the average number of sulfate groups per disaccharide unit, or net sulfation, of CS/DS isomers is a useful index of ECM physiochemical properties. For example, an increase in sulfate groups per disaccharide unit ('hypersulfation') was recently reported in the brain of patients with Alzheimer's disease.[28] Whether IBD associates with similar changes in the intestinal CS/DS-GAG isomer profile remains to be determined, but based upon the above considerations, we hypothesized that a hypersulfated, pro-inflammatory CS/DS-GAG isomer composition would compromise mucous barrier function, interfere with glycan-lectin interactions, and alter mucosal immunity and gut microbiota[41–44] in ways that associate with active IBD.

Similarly, the question of whether the CS/DS isomer composition is altered by effective IBD therapy also remains unknown, nor has a detailed analysis of CS/DS-GAG sulfation pattern in the human intestine been reported. In the current work, we employ a sensitive and accurate mass spectrometry method[28,32] to analyze the intestinal CS/DS-GAG sulfation code in healthy pediatric and adult patients without intestinal inflammation. We then compare these data to the CS/DS-GAG sulfation code in cohorts of pediatric patients both with active, untreated IBD and with IBD in CR. Our goal was to characterize whether areas of inflamed bowel exhibit increased pro-inflammatory CS/DS isomers and decreased pro-stabilizing CS/DS

isomers and explore the role of pro-inflammatory changes in the composition of the intestinal ECM in IBD pathogenesis.

RESULTS

Intestinal CS/DS-GAG composition in pediatric patients without intestinal inflammation

The relative abundance of each of the five intestinal CS/DS isomers, which comprises the intestinal CS/DS-GAG 'sulfation code,' was determined by mass spectrometry from 13 healthy pediatric/young adult patients without intestinal inflammation (Table 1, age range 12–23) in the duo (n = 6), TI (n = 7), and left colon (n = 13) is shown in Fig. 2a. Consistent with what is observed in other tissues (*e.g.*, brain[28]), the abundance of CS-A was consistently higher than any other isomer throughout the gastrointestinal tract (Fig. 2a). There was no hypersulfation present, with the average number of sulfate groups per CS isomer remaining near 1.0 irrespective of intestinal location (Fig. 2b; duo vs TI 1.009 vs 0.999, p = 0.331; duo vs colon 1.009 vs 0.999, p = 0.218; TI vs colon 0.999 vs 0.999, p = 0.999).

Table 1

Patient demographics. Intestinal biopsy samples from 13 pediatric control patients, 6 adult control patients, 15 pediatric patients with ulcerative colitis (UC) or indeterminant colitis, and 22 pediatric patients with Crohn's disease (CD) were included in the study. Montreal classification was used to categorize CD phenotype. ADA = adalimumab, IFX = infliximab, Mono = monotherapy, IMM = immunomodulator (methotrexate, 6-mercaptopurine, or azathioprine), VDZ = vedolizumab, Mesal = mesalamine/5-amino salicylic acid, MTX = methotrexate, SCD = Specific Carbohydrate Diet.

	Pediatric control	Adult control	Pediatric ulcerative colitis (Includes 1 patient with indeterminant colitis)	Pediatric Crohn's disease (with colonic involvement at diagnosis)
No. of patients	13	6	15	22
Age at scope, years (mean, range)	16.7 (12−23)	36.3 (24−67)	13.9 (7−18)	13.3 (9−18)
Sex (% female)	6/13 (46.2%)	3/6 (50.0%)	6/15 (40.0%)	7/22 (31.8%)
IBD phenotype	-	-	Pancolitis: 13/15 (86.7%) Left sided colitis: 1/15 (6.7%) Unspecified: 1/15 (6.7%)	L2B1: 2/22 (9.1%) L2L4B1: 2/22 (9.1%) L3B1: 14/22 (63.6%) L3B1 + p: 1/22 (4.5%) L3B2: 1/22 (4.5%) L3L4B1: 2/22 (9.1%)
No. of follow up scopes on therapy	-	-	9	13

	Pediatric control	Adult control	Pediatric ulcerative colitis (Includes 1 patient with indeterminant colitis)	Pediatric Crohn's disease (with colonic involvement at diagnosis)
Therapy at follow up scope	-	-	ADA: 2/9 (22.2%)	ADA: 8/13 (61.5%)
			IFX: 2/9 (22.2%)	Mono: 4/13 (30.7%)
			Mono: 0	+IMM: 4/13 (30.7%)
			+IMM: 2/9 (22.2%)	IFX: 2/13 (15.3%)
			VDZ: 3/9 (33.3%)	Mono: 2/13 (15.3%)
			Mesal: 2/9 (22.2%)	MTX: 6/13 (46.2%)
			7/9 (77.8%) on a biologic	Mono: 1/13 (7.7%)
				+SCD: 1/13 (7.7%)
				+ADA: 4/13 (30.7%)
				SCD: 2/13 (15.3%)
				Mono: 1/13 (7.7%)
				+MTX: 1/13 (7.7%)
				10/13 (76.9%) on a biologic

The relative abundance of CS-A increased from proximal to distal intestine, with mean values ranging from 65.5% in the duo to 76.5% in the colon (Fig. 2c). CS-C was the second most abundant isomer found throughout the intestines and was relatively less abundant in the colon than the small intestine, with mean values ranging from 26.4% in the duo to 18.1% in the colon (Fig. 2d). Each of the remaining isomers (CS-O, CS-E, and DS) comprised < 5% of total CS isomer total throughout the intestine (Fig. 2e-g; CS-O: Duo 3.6%, TI 4.4%, Colon 2.7%; CS-E: Duo 3.5%, TI 2.8%, Colon 1.5%; DS: Duo 1.1%, TI 1.5%, Colon 1.2%).

Of the 13 patients without any gross or histologic abnormalities on endoscopic evaluation, 4 of these patients were truly healthy controls (HC) (aged 18–23) who were paid to undergo endoscopy without any GI symptoms present, while 9 were patients who had GI symptoms that prompted endoscopic evaluation (usually abdominal pain), termed functional GI disease (FGID). There were no significant differences in CS/DS-GAG isomer profiles in the colon detected between HC and FGID individuals (**Supplemental Fig. S1**). Given the lack of significant differences in CS/DS-GAG profiles in the colon, both HC and FGID patients are included as controls for comparison to patients with IBD.

CS/DS isomer abundance by age in patients without intestinal inflammation

To investigate whether human intestinal CS/DS-GAG composition is affected by age, we compared isomer patterns from the colons of a subset of adult patients (Table 1, n = 6, age range 24–67) to those of pediatric patients without IBD described above. This analysis showed no significant correlation between patient age and the abundance of any individual CS/DS isomer (Fig. 2h; mean isomer percentages across all ages and p-value of linear regression: CS-A 76.4% (p = 0.389), CS-C 17.7% (p = 0.810), CS-O 3.1% (p = 0.070), CS-E 1.6% (p = 0.282), DS 1.2% (p = 0.612)).

Patients with active IBD demonstrate significantly altered CS/DS-GAG composition in involved bowel

Next, we compared mass spectrometry analysis of CS/DS isomer composition of colonic mucosal samples obtained from a cohort of pediatric patients with active IBD with colonic involvement at diagnosis before therapy was initiated (UC and CD colitis/ileocolonic disease, n = 22) to values obtained from healthy pediatric controls (Fig. 3a). These patients had both active clinical IBD symptoms (PUCAI/PCDAI > 10) and endoscopic and histologic evidence of chronic and/or active inflammation on biopsies from the left colon. Most patients with UC had pancolitis (Table 1), while most patients with CD had non-penetrating, non-stricturing ileocolonic disease based on the Montreal classification (Table 1). In pediatric patients with IBD at diagnosis, we found a significantly reduced abundance of the two pro-stabilizing isomers, CS-A (Fig. 3b, 76.5% vs 70.3%, p < 0.0001) and DS (Fig. 3c, 1.2% vs 0.7%, p < 0.0001). By comparison, CS-O, the non-sulfated isomer, was not significantly altered in patients with active IBD (Fig. 3d, 2.7% vs 3.0%, p = 0.77), while the abundance of the two pro-inflammatory isomers CS-C (Fig. 3e, 18.1% vs 21.9%, p = 0.0015) and CS-E (Fig. 3f, 1.5% vs 4.1%, p < 0.0001) were increased. The net effect of these observed CS/DS-GAG changes was an overall hypersulfation of the CS/DS-GAG profile in the colon in patients with active IBD compared to controls (Fig. 3g, average sulfates per disaccharide unit 0.999 vs 1.019, p = 0.0005), driven primarily by a marked increase in the disulfated pro-inflammatory CS-E isomer (Fig. 3f). Overall, pediatric patients with active IBD at diagnosis with colonic involvement show pathologic alterations in their CS/DS-GAG sulfation code that favor a more inflammatory and less stable matrix composition compared to individuals without IBD.

IBD treatments that achieve CR reverse the CS/DS-GAG profile changes found in active IBD to match controls

CS/DS isomer composition was then characterized in patients with IBD who had colonic disease at diagnosis who subsequently had biopsies taken from the left colon on restaging endoscopy while in CR (PUCAI or PCDAI score < 10) (n = 22). Most of these patients at follow up in CR were on biologic therapies (Table 1, 77.8% of UC patients and 76.9% in CD patients). In IBD in CR, the altered CS-GAG isomer profiles seen in patients with active disease were largely reversed, such that their isomer compositions closely matched those of controls (Fig. 3a). Specifically, compared to IBD patients at diagnosis, IBD patients in CR had an increase in the pro-stabilizing isomers CS-A (Fig. 3b, 70.3% vs 77.6%, p < 0.0001) and DS (Fig. 3c, 0.7% vs 1.0%, p = 0.004). Conversely, the abundance of the two pro-inflammatory isomers were

decreased in IBD patients in CR, including CS-C (Fig. 3e, 21.9% vs 16.6%, p < 0.0001) and CS-E (Fig. 3f, 4.1% vs 2.5%, p = 0.001), when compared to IBD patients at diagnosis with clinically active disease.

Notably, the colonic isomer abundance profiles of IBD patients in CR nearly phenocopy those of control patients (Fig. 3a), with the exception that DS was slightly lower in IBD patients in CR than in controls (Fig. 3c, DS: 1.2% vs 1.0%, p = 0.042). CS-E appears slightly higher in IBD patients in CR than in controls, but it does not reach statistical significance (Fig. 3f, CS-E: 2.5% vs 1.5%, p = 0.089). Furthermore, when the isomer profile of these 22 patients with colonic IBD in CR were compared to the subset of patients who were in endoscopic remission, defined as absence of gross and histologic inflammation on endoscopic evaluation (n = 14), there were no significant differences in CS/DS isomer composition (**Supplemental Fig. S2**). These findings suggest that effective normalization of the CS/DS isomer composition is more dependent on CR rather than mucosal healing.

Nevertheless, the hypersulfation characteristic of intestinal CS/DS isomers in active IBD remained detectable in patients in CR. Specifically, the mean number of sulfate groups per CS/DS-disaccharide in patients with IBD in CR remained elevated compared to controls (Fig. 3g, Control vs IBD in CR: 0.999 vs 1.014, p = 0.011). This effect appears to reflect the less dramatic reversal of elevated disulfated CS-E content in patients in CR compared to controls.

CS/DS-GAG sulfation patterns correlate with histologic and clinical IBD activity

Beyond the demonstration that pro-stabilizing CS/DS isomers (CS-A and DS) are reduced in the intestine of patients with active IBD, we also found that the abundance of these isomers decreases in proportion to the degree of histologic inflammation present in the colon (Fig. 4a,b). Thus, levels of CS-A and DS were lower in patients with moderate/severe colonic inflammation than in patients with lesser degrees of inflammation (Fig. 4a CS-A: none vs moderate/severe, p < 0.0001, none vs mild, p = 0.002; Fig. 4b DS: none vs moderate/severe, p < 0.0001, none vs mild, p = 0.002). Conversely, the abundance of pro-inflammatory isomers (CS-C and CS-E) increased in proportion to the degree of histologic inflammation present in the colon (Fig. 4c CS-C: none vs moderate/severe, p < 0.0001, none vs mild, p = 0.096; Fig. 4d CS-E: none vs moderate/severe, p = 0.0002, none vs mild, p = 0.007).

In addition to the correlation between CS/DS isomer sulfation patterns and histologic IBD activity, we also identified a significant correlation between CS/DS isomers and clinical IBD activity. Clinical IBD activity in patients with IBD with colonic disease, as defined by the PUCAI score for UC patients or the PCDAI score for CD patients, inversely correlated with the abundance of pro-stabilizing isomers (Fig. 4e, f), and positively correlated with the abundance of pro-inflammatory isomers (Fig. 4g, h). Specifically, CS-A inversely correlated with PUCAI/PCDAI scores (Fig. 4e, p < 0.0001, R^2 = 0.598) as did DS (Fig. 4f, p < 0.0001, R^2 = 0.340), while mean levels of CS-C and CS-E each showed a significant positive correlation with PUCAI/PCDAI scores (Fig. 4g, CS-C: p < 0.0001, R^2 = 0.467; Fig. 4h, CS-E: p = 0.003, R^2 = 0.234). Based on this analysis, there seems to be a threshold effect with respect to the abundance of the certain

isomers. Namely, when the abundance of CS-A was above 77%, PUCAI/PCDAI scores only range from 0–5 (Fig. 4e), suggesting that CS-A abundance above this threshold can serve as a predictor of CR. Conversely, when the abundance of pro-inflammatory CS-C is above 21% (Fig. 4g), PUCAI/PCDAI scores are > 10, implying that a CS-C abundance above this threshold can serve as a predictor of active clinical IBD symptoms.

DISCUSSION

Using a novel mass spectrometry method, we report the CS/DS-GAG composition, or sulfation code, of the human intestine. To our knowledge, this analysis has not previously been reported, nor has our finding that relative to healthy controls, the intestinal CS/DS-GAG composition differs significantly in pediatric and young adult patients with active colonic IBD. Specifically, we report that in active IBD, pro-inflammatory isomers are increased and stabilizing matrix isomers are decreased, a pattern that is largely reversed upon achieving CR with IBD therapy. We also show that in patients with active IBD, the magnitude of these changes in intestinal CS/DS-GAG composition varies in proportion to disease severity, based on clinical as well as histochemical criteria. Although causality cannot be inferred from these relationships, our findings are consistent with a model whereby IBD pathogenesis involves pathological changes in ECM composition, and future studies are warranted to test this hypothesis.

The pattern created by repeating CS/DS isomers bound to core proteins such as aggrecan in the ECM creates a sulfation code that influences many cellular processes and can potentially contribute the pathogenesis of specific diseases.[45–47] A key goal of the current work was to report the sulfation code of the intestines for the first time. We found that in young individuals with endoscopically and histologically normal intestinal tissue, CS-A is by far the most abundant isomer, and this predominance increases as one moves from the small intestine to in the colon. Conversely, the abundance of CS-C, the second most abundant isomer, is higher in proximal small bowel than terminal ileum or colon. Stated differently, the ratio of CS-C to CS-A increases as one moves distally from the proximal small bowel to the colon. Although the functional significance of this pattern requires additional study, it may reflect a permissive role for CS-C to facilitate epithelial cell turnover, a process that is more rapid in small intestine than colon.[48,49] Furthermore, the flatter mucosal surface of the colonic epithelium, where CS-A content is highest, may benefit from a less plastic and more stable network of CS/DS isomers compared to the villous structure of the small intestine. Additional studies are warranted to investigate these possibilities, as well as the potential impact on CS/DS isomer profiles of gut microbiota, including bacteria that express chondroitinase enzymes that digest CS/DS-GAGs,[50] which are likely more abundant in colon than the small intestine.

Next, we sought to determine how the intestinal CS/DS-GAG profile is impacted in patients with clinical IBD symptoms and active IBD mucosal inflammation. This work was motivated in part by evidence of a role for aberrant CS/DS-GAG composition in the pathogenesis and progression of IBD. Specifically, the overall abundance of CS/DS-GAGs has been shown to be reduced in intestinal samples from patients with UC and CD compared to controls, and the areas of bowel with the highest GAG disruption have been

shown to correlate with the highest concentration of macrophages that are positive for tumor necrosis factor alpha (TNF), a key mediator of the abnormal immune response implicated in the pathogenesis of IBD.[51] Pathological changes in the composition of specific CS/DS isomers is also reported in other disease states, including Alzheimer's dementia, spinal cord injury, and cardiac reperfusion injury.[28,52–54] We therefore sought to determine whether the CS/DS-GAG sulfation signature is altered in association with mucosal IBD lesions. Relative to healthy control tissue, we found marked differences in the CS/DS-GAG profile of mucosal biopsies taken from individuals with both active IBD symptoms at diagnosis and evidence of endoscopic and histologic inflammation. Specifically, the abundance of pro-inflammatory isomers CS-C and CS-E were increased in IBD mucosal lesions, while that of pro-stabilizing isomers CS-A and DS was decreased.

One potential confounding factor in comparing the CS/DS isomer profile in control patients to individuals with IBD is that our control population tended to be somewhat older. To address this concern, we investigated whether CS/DS isomer composition varied by age in normal subjects. We report that in healthy patients ranging in age from 12 to 67, intestinal CS/DS isomer composition did not vary significantly with age. It is therefore unlikely that the differences in CS/DS isomer profiles observed between our control patients and patients with IBD were confounded by an effect of age. This is distinct from our current knowledge about CS/DS-GAG sulfation patterns in the brain, which are shown to change throughout the lifespan as the brain matrix "stiffens" with age and becomes less plastic,[32] implying that the intestinal matrix maturation process is complete by early adolescence. Further studies are needed to investigate the intestinal CS/DS-GAG profiles in younger individuals to determine the "critical period" for ECM maturation in the intestines.

We next sought to determine whether these CS/DS-GAG sulfation code changes represent an underlying predisposition to IBD or instead are features of active disease. To this end, we compared the sulfation signature among individuals with IBD in CR at restaging endoscopic evaluation while on effective IBD therapy to that of patients with active IBD at diagnosis. This analysis revealed that in patients in CR, the ratio of pro- and anti-inflammatory isomers was restored to a value similar to that of healthy controls. Therefore, the observed changes in the isomer profiles appear to develop only in the setting of active IBD pathology and do not represent an underlying predisposition to developing disease. Furthermore, compared to patients in CR, patients in true ER who achieve deep mucosal healing show no significant CS/DS isomer profile changes, which suggests that the CS/DS isomer composition is not merely a byproduct of active inflammation but is related to IBD symptomatology and is altered by effective IBD treatments.

Notably, although the CS/DS isomer composition in individuals with IBD in CR at follow up is similar to that of controls, there is persistent hypersulfation present even when CR is achieved, mostly driven by a less dramatic reduction in the pro-inflammatory disulfated CS-E isomer (4S6S). The degree of sulfation therefore may serve as a disease biomarker. Further studies are warranted to follow individuals longitudinally and determine whether the degree of sulfation or the abundance of CS-E is associated with a higher likelihood of disease relapse. Our results also point to a threshold abundance of CS-A above 77%

as predictive of CR. CS-A abundance, therefore, may serve as a biomarker for response to therapy and sustained CR, although additional studies are indicated to probe this association further. There is clear potential for the CS/DS-GAG sulfation signature to serve as a disease biomarker in IBD, which can guide treatment decisions and timing of repeat endoscopic evaluation.

A key question raised by these findings is whether observed changes in CS/DS isomer composition contribute to IBD pathology and are therefore also a potential therapeutic target, or instead are only a byproduct of active IBD inflammation. While additional work is needed to establish causality, it is noteworthy that the abundance of pro-stabilizing CS/DS isomers (CS-A and DS) correlated inversely with both pathologic severity and clinical IBD scores, while the abundance of pro-inflammatory isomers (CS-C and CS-E) correlated positively with these markers of IBD activity. These observations are suggestive of an intricate link between altered intestinal ECM structure and function (and CS/DS isomers, in particular) and the underlying disease process. Preclinical data from rodent studies provides further support that CS as part of the ECM plays an active role in IBD. Specifically, in rats, oral CS administration (a combination of CS isomers, predominantly CS-A), improves clinical and histologic outcomes in a dextran sodium sulfate colitis (DSS) model of IBD.[55] Notably, this effect was more robust and effective compared to animals receiving 5-aminosalysilic acid administration, a current first line therapy for mild to moderate UC.[55] Additionally, DSS colitis outcomes in mice were found to be improved in response to an siRNA-based strategy that altered sulfotransferase enzymatic activity, thereby reducing the abundance of pro-inflammatory CS-E in the colon.[36] Similar outcomes are reported in cardiac tissue, where targeted administration of the stable DS isomer following a cardiac ischemic event was effective in preventing reperfusion inflammation injury.[54]

In summary, our mass spectrometry analysis decodes the CS/DS-GAG sulfation signature of the human intestine for the first time and reveals pathogenic changes of CS/DS-GAG composition in areas of inflamed bowel in IBD, with pro-inflammatory isomers displacing pro-stabilizing isomers. As these ECM changes are both strongly associated with disease activity and reversed by effective IBD treatment, a priority for future studies is to determine 1) the extent to which reversal of pathogenic intestinal ECM compositional changes can improve IBD outcomes without immunosuppression, and 2) whether the intestinal CS/DS-GAG sulfation signature can be monitored as a biomarker of IBD activity.

METHODS

Patient selection

Intestinal biopsy samples from pediatric and young adult patients with and without IBD were obtained from deidentified, banked samples through the PREDICT, ISTAT, and LAND-HO studies (PREDICT IRB STUDY00001017, ISTAT IRB STUDY00001308, and LAND-HO IRB STUDY00002018). Experiments were approved by Seattle Children's Hospital and University of Washington Institutional Review Boards. All methods were carried out in accordance with relevant guidelines and regulations. Because all tissue samples and corresponding clinical information (age and gender for all patients, and diagnosis, IBD

medical therapy, and PUCAI/PCDAI scoring for patients with IBD) were de-identified, informed consent was not necessary. While this was primarily a pediatric focused analysis, young adults between 18–23 were included as healthy controls because they could give their own consent to participate as healthy endoscopy subjects. We included all control biopsy samples that were available from these studies, and for patients with IBD our inclusion criteria were: biopsies taken from patients at time of diagnosis who were confirmed to have IBD who had clinically active symptoms and were not on treatment, with gross endoscopic and histologic colonic involvement, and/or biopsies from patients with IBD who had colonic involvement (endoscopically and histologically) at diagnosis who had subsequent biopsies taken on restaging evaluation on therapy while in CR. Most of these patients at time of follow up in CR were also in biochemical remission, with normal erythrocyte sedimentation rate and C-reactive protein lab values, but this was not an inclusion criterion for this study. There were relatively few patients who had a fecal calprotectin collected at the same time as endoscopic evaluation, so this was also not used as an inclusion criterion. A total of 50 pediatric/young adult patients were included: 13 control patients, and 37 with IBD with colonic disease who met the above inclusion criteria (14 patients with ulcerative colitis, 1 patient with indeterminant colitis, and 22 with Crohn's disease). A smaller set of colonic biopsies from 6 deidentified adult control patients without IBD obtained through the University of Washington Gastrointestinal Center for Analytical Research and Exploratory Science (GICaRes) Biorepository (IRB 34095/2161) was also included for comparison to the pediatric population. All human tissue samples used in the analysis were deidentified, and the clinical information was provided for each deidentified sample.

Pathologic and clinical IBD assessment

Researchers had access to pathology reports from each patient at the time of tissue collection/endoscopic evaluation. The degree of histological inflammation was categorized into none, mild, moderate, or severe according to the language used in the original pathology reports. Because relatively few patients had severe inflammation, moderate and severe groups were combined in our analysis.

Clinical IBD activity scores, specifically the pediatric ulcerative colitis activity index (PUCAI)[56] and pediatric Crohn's disease activity index (PCDAI) scores,[57] were calculated for each patient at the time of endoscopic evaluation based on retrospective chart review. When a numeric score was not explicitly mentioned in the chart, scores were retroactively calculated using available clinical and anthropometric information. Patients were considered to have active disease if PUCAI/PCDAI score was greater than 10. PUCAI/PCDAI scores from 10–34 were considered mild disease, 35–64 as moderate disease, and 65 or greater as severe disease.

Intestinal tissue processing

Intestinal biopsy samples from the duodenum (duo), terminal ileum (TI), and left/rectosigmoid colon were formalin-fixed and paraffin embedded (FFPE) and 4μm thick sections were cut and mounted onto slides. FFPE sections were de-waxed using xylenes (Thermo Fischer Scientific, 1330-20-07, Waltham, MA)

and a series of graded ethanol washes. Slides were then washed in phosphate buffered saline followed by 3x in Optima liquid chromatography/mass spectrometry (LC/MS)-grade water (Thermo Fisher Scientific, 7732-18-5, Waltham, MA) and 1x in 50mM ammonium bicarbonate (pH 7.6; Sigma, 09830, Burlington, MA) at room temperature. Chondroitinase ABC (ChABC) enzyme (Sigma, C3667, Burlington, MA), a combinatorial lyase/enolase that selectively degrades all CS/DS-GAG chains into individual isomers, or disaccharide units,[58,59] was reconstituted at a concentration of 500mU/mL in 50mM ammonium bicarbonate (pH 7.6). Using a hydrophobic pen to outline the tissue sections on each slide, reconstituted ChABC enzyme was added to cover each tissue section (200-500μL per slide depending on tissue surface area), and slides were incubated at 37°C in a Thermo Fisher Scientific MaxQ4000 orbital shaker for 24 hours. Afterward, the liquid incubation media was collected and spun at 14,000g for 10 minutes at room temperature to remove any tissue debris. The supernatant was collected and then dehydrated using a Thermo Fisher Scientific SpeedVac Concentrator and the resulting product was reconstituted in 30μL of LC/MS-grade water for liquid chromatography with tandem mass spectrometry (LC-MS/MS) analysis. Figure 1d outlines the tissue processing workflow for the intestinal biopsy samples.

LC-MS/MS quantification of isolated CS isomers

After isolating CS/DS isomers (disaccharide units) from duo, TI, and colon tissues as outlined above, samples were analyzed using a triple quadropole mass spectrometer equipped with electrospray ion source (Waters Xevo TQ-S, Milford, MA) operated in negative mode ionization. LC-MS/MS was performed using a Waters Acuity I-class ultraperformance liquid chromatographic system (UPLC) coupled to the Waters Xevo TQ-S system. A Hypercarb column (2.1 Å~50mm, 3μm; Thermo Fisher Scientific, Waltham, MA) was used to resolve the isomers as described previously,[32] assigning the following multiple reaction monitoring (MRM) channels: DDS (2S4S-DS) and DE (4S6S-CS), m/z 538 > 300; DA (4S-CS), m/z 458 > 300; DO (0S-CS) m/z 378 > 175; and DC (6S-CS) m/z 458 > 282. Data was acquired and quantified using MassLynx software version 4.1 (Waters, Milford, MA). Using the MRM channels described above, the ratios between peak areas resulting from equimolar CS/DS standard mixes were normalized to the highest peak intensity and relative quantification of each isomer within a sample was achieved using a modified peak area normalization function as previously described.[32] Each sample of tissues were normalized using internal control samples that were repeated in each LC-MS/MS run. Each CS/DS isomer was expressed as a percentage of the relative abundance of each CS/DS isomer within an intestinal sample, which allowed us to account for any variation in absolute tissue size from the biopsy samples. The average number of sulfates per DCS (sulfation) was computed using the following formula:

$$Avg\#S/\Delta CS = \sum_{(i=1)}^{n} (x_i + w_i)/ \sum_{(i=1)}^{n} w_i \quad x_i = \#Sulfates(0 - 2)$$

$$w_i = percent\ \Delta\ CS$$

Statistical analysis

A mixed-effects, repeated measures two-way analysis of variance (ANOVA) with matched CS/DS isomers and intestinal regions was used for the primary analysis comparing CS/DS isomer compositional changes between intestinal locations and between individuals without intestinal inflammation, patients with active IBD, and IBD in remission in Fig. 2a and 3a. To compare individual isomer abundance or sulfation between each bowel location in Fig. 2b-g, a secondary analysis using Tukey's multiple comparisons test was conducted to compare individual isomer abundance between each group and each bowel location. Data from colon biopsies for each isomer in control patients was normally distributed. To compare individual isomer abundance between controls groups and IBD groups in Fig. 3b-g, a one-way ANOVA using Tukey's multiple comparisons test was used for normally distributed data (CS-A, DS, and CS-C). A Kruskal-Wallis nonparametric test was used for data that was not normally distributed (CS-O, CS-E, and sulfation). To compare the severity of histologic inflammation for each isomer in Fig. 4a-d, Tukey's multiple comparisons test was used for normally distributed data (DS, CS-C, and CS-E), and a Kruskal-Wallis test was used for data that was not normally distributed (CS-A). Normality (i.e. Gaussian distribution) was tested for using the D'Agostino-Pearson test using an alpha value of 0.05.

Whether the abundance of each isomer varied with disease activity was determined by linear regression (the 95% confidence interval bands of the best-fit line was used to compare each individual CS/DS isomer to the corresponding clinical IBD severity scores). R^2 analysis was also used to determine the extent to which variance in CS/DS isomer abundance was attributable to variation in IBD severity. GraphPad Prism 9.0 (Graph Pad Software Inc., La Jolla, CA) was used to complete statistical analyses. Error bars represent the standard error of the mean. All differences were considered statistically significant at $p < 0.05$. An alpha value of 0.05 was used for all analyses. Investigators were blinded to group conditions during quantitative mass spectrometry analysis.

Declarations

Author Contributions: KLF, KMA, and JMS conceived the idea behind the study, and KLF and KMA carried out the experiment and were responsible for data collection, analysis, and interpretation. HZ, DLS, and MN were responsible for providing de-identified intestinal biopsy samples for the study. BAP helped with sample processing and data collection. KLF was responsible for drafting the article, and KMA, MWS,

GJM, JMS, HZ, DLS, MN, AH, and BAP were responsible for revising and editing to help create the final version of the manuscript.

Data availability: All data are presented in the article and can be further requested from the corresponding author.

Additional information: The authors declare no competing interests.

References

1. Atlab, S. *et al.* The global, regional, and national burden of inflammatory bowel disease in 195 countries and territories, 1990–2017: a systematic analysis for the Global Burden of Disease Study 2017. Lancet Gastroenterology Hepatology 5, 17–30 (2019).

2. Chudy-Onwugaje, K. O., Christian, K. E., Farraye, F. A. & Cross, R. K. A State-of-the-Art Review of New and Emerging Therapies for the Treatment of IBD. Inflamm. Bowel Dis. 25, 820–830 (2018).

3. Villablanca, E. J., Selin, K. & Hedin, C. R. H. Mechanisms of mucosal healing: treating inflammatory bowel disease without immunosuppression? Nat. Rev. Gastroenterol. 19, 493–507 (2022).

4. Cai, Z., Wang, S. & Li, J. Treatment of inflammatory bowel disease: a comprehensive review. Frontiers Medicine 8, 765474 (2021).

5. Lichtenstein, G. R. *et al.* ACG clinical guideline: management of Crohn's disease in adults. Am. J. Gastroenterol. 113, 481–517 (2018).

6. Worley, G. *et al.* Colectomy rates for ulcerative colitis in England 2003-2016. Aliment. Pharm. Therap. 53, 484–498 (2021).

7. Yang, E. *et al.* Efficacy and safety of simultaneous treatment with two biologic medications in refractory Crohn's disease. Aliment. Pharm. Therap. 51, 1031–1038 (2020).

8. Chambrun, G. P. de, Peyrin-Biroulet, L., Lémann, M. & Colombel, J.-F. Clinical implications of mucosal healing for the management of IBD. Nat. Rev. Gastroenterol. 7, 15–29 (2010).

9. Ungaro, R. C. *et al.* Deep remission at one year prevents progression of early Crohn's disease. Gastroenterology 159, 139–147 (2020).

10. Carvalho, P. B. & Cotter, J. Mucosal healing in ulcerative colitis: a comprehensive review. Drugs 77, 159–173 (2017).

11. Neurath, M. F. New targets for mucosal healing and therapy in inflammatory bowel diseases. Mucosal Immunol. 7, 6–19 (2014).

12. Guan, Q. A comprehensive review and update on the pathogenesis of inflammatory bowel disease. *J. Immunol. Res.* 2019, 7247238 (2019).

13. Zhang, Y.-Z. & Li, Y.-Y. Inflammatory bowel disease: pathogenesis. World J Gastroenterol. 20, 91–99 (2014).

14. Xavier, R. J. & Podolsky, D. K. Unravelling the pathogenesis of inflammatory bowel disease. Nature 448, 427–434 (2007).

15. Chang, J. *et al.* Impaired intestinal permeability contributes to ongoing bowel symptoms in patients with inflammatory bowel disease and mucosal healing. Gastroenterology 153, 723–731.e1 (2017).

16. Kang, Y., Park, H., Choe, B.-H. & Kang, B. The role and function of mucins and its relationship to inflammatory bowel disease. Frontiers Medicine 9, 848344 (2022).

17. d'Aldebert, E. *et al.* Characterization of human colon organoids from inflammatory bowel disease patients. Frontiers Cell. Dev. Biology 8, 363 (2020).

18. Golusda, L., Kühl, A. A., Siegmund, B. & Paclik, D. Extracellular matrix components as diagnostic tools in inflammatory bowel disease. Biology 10, 1024 (2021).

19. Petrey, A. C. & Motte, C. A. de la. The extracellular matrix in IBD. *Curr. Opin. Gastroenterol.* 33, 234–238 (2017).

20. Derkacz, A., Olczyk, P., Olczyk, K. & Komosinska-Vassev, K. The role of extracellular matrix components in inflammatory bowel diseases. J. Clin. Medicine 10, 1122 (2021).

21. Pompili, S., Latella, G., Gaudio, E., Sferra, R. & Vetuschi, A. The charming world of the extracellular matrix: a dynamic and protective network of the intestinal wall. Frontiers Medicine 8, 610189 (2021).

22. Derkacz, A., Olczyk, P., Jura-Półtorak, A., Olczyk, K. & Komosinska-Vassev, K. The diagnostic usefulness of circulating profile of extracellular matrix components: sulfated glycosaminoglycans (sGAG), hyaluronan (HA) and extracellular part of Syndecan-1 (sCD138) in patients with Crohn's disease and ulcerative colitis. J. Clin. Medicine 10, 1722 (2021).

23. Kechagia, J. Z., Ivaska, J. & Roca-Cusachs, P. Integrins as biomechanical sensors of the microenvironment. Nat. Rev. Mol. Cell Bio. 20, 457–473 (2019).

24. Asano, K., Yoshimura, S. & Nakane, A. Alteration of intestinal microbiota in mice orally administered with salmon cartilage proteoglycan, a prophylactic agent. PLoS ONE 8, e75008 (2013).

25. Sashinami, H. *et al.* Salmon proteoglycan suppresses progression of mouse experimental autoimmune encephalomyelitis via regulation of Th17 and Foxp3 + regulatory T cells. Life Sci. 91, 1263–1269 (2012).

26. Kudo, K., Kobayashi, T., Kasai, K., Nozaka, H. & Nakamura, T. Chondroitin sulfate is not digested at all in the mouse small intestine but may suppress interleukin 6 expression induced by tumor necrosis factor-α. Biochem. Biophys. Res. Commun. 642, 185–191 (2023).

27. Mortensen, JH. *et al.* The intestinal tissue homeostasis – the role of extracellular matrix remodeling in inflammatory bowel disease. Expert Rev. Gastroent. 13, 1–17 (2019).

28. Logsdon, A. F. *et al.* Decoding perineuronal net glycan sulfation patterns in the Alzheimer's disease brain. Alzheimer's Dementia 18, 942–954 (2021).

29. Scarlett, J. M., Hu, S. J. & Alonge, K. M. The "loss" of perineuronal nets in Alzheimer's disease: missing or hiding in plain sight? Front. Integr. Neurosci. 16, 896400 (2022).

30. Alonge, K. M. *et al.* Hypothalamic perineuronal net assembly is required for sustained diabetes remission induced by fibroblast growth factor 1 in rats. Nat. Metab. 2, 1025–1033 (2020).

31. Miyata, S. & Kitagawa, H. Chondroitin 6-sulfation regulates perineuronal net formation by controlling the stability of aggrecan. *Neural Plast.* 2016, 1–13 (2016).

32. Alonge, K. M. *et al.* Quantitative analysis of chondroitin sulfate disaccharides from human and rodent fixed brain tissue by electrospray ionization-tandem mass spectrometry. Glycobiology 29, 847–860 (2019).

33. Djerbal, L., Lortat-Jacob, H. & Kwok, J. Chondroitin sulfates and their binding molecules in the central nervous system. Glycoconjugate J 34, 363–376 (2017).

34. Mizumoto, S. & Yamada, S. The specific role of dermatan sulfate as an instructive glycosaminoglycan in tissue development. Int. J. Mol. Sci. 23, 7485 (2022).

35. Rizzo-Valente, V. S. *et al.* Effects of dermatan sulfate from marine invertebrate Styela plicata in the wound healing pathway: a natural resource applied to regenerative therapy. Mar. Drugs 20, 676 (2022).

36. Suzuki, K. *et al.* Pivotal role of carbohydrate sulfotransferase 15 in fibrosis and mucosal healing in mouse colitis. Plos One 11, e0158967 (2016).

37. Ohtake, S. *et al.* Expression of sulfotransferases involved in the biosynthesis of chondroitin sulfate E in the bone marrow derived mast cells. Biochem. Biophys. Acta (BBA) - Gen. Subj. 1780, 687–695 (2008).

38. Habuchi, O., Moroi, R. & Ohtake, S. Enzymatic synthesis of chondroitin sulfate E by N-acetylgalactosamine 4-sulfate 6-O-sulfotransferase purified from squid cartilage. Anal. Biochem. 310, 129–136 (2002).

39. Gilbert, R. J. *et al.* CS-4,6 is differentially upregulated in glial scar and is a potent inhibitor of neurite extension. Mol. Cell. Neurosci. 29, 545–558 (2005).

40. Syková, E. & Nicholson, C. Diffusion in brain extracellular space. Physiol. Rev. 88, 1277–1340 (2008).

41. Kudelka, M. R., Stowell, S. R., Cummings, R. D. & Neish, A. S. Intestinal epithelial glycosylation in homeostasis and gut microbiota interactions in IBD. Nat. Rev. Gastroenterol. 17, 597–617 (2020).

42. Bergstrom, K. *et al.* Defective intestinal mucin-type O-glycosylation causes spontaneous colitis-associated cancer in mice. Gastroenterology 151, 152–164.e11 (2016).

43. Rausch, P. *et al.* Colonic mucosa-associated microbiota is influenced by an interaction of Crohn disease and FUT2 (Secretor) genotype. *Proc. National Acad. Sci.* 108, 19030–19035 (2011).

44. Fu, J. *et al.* Loss of intestinal core 1–derived O-glycans causes spontaneous colitis in mice. J. Clin. Invest. 121, 1657–1666 (2011).

45. Testa, D., Prochiantz, A. & Nardo, A. A. D. Perineuronal nets in brain physiology and disease. Semin. Cell Dev. Biol. 89, 125–135 (2018).

46. Morawski, M. *et al.* Involvement of perineuronal and perisynaptic extracellular matrix in Alzheimer's disease neuropathology. Brain Pathol. 22, 547–561 (2012).

47. Pantazopoulos, H. & Berretta, S. In sickness and in health: perineuronal nets and synaptic plasticity in psychiatric disorders. *Neural Plast.* 2016, 1–23 (2016).

48. Darwich, A. S., Aslam, U., Ashcroft, D. M. & Rostami-Hodjegan, A. Meta-analysis of the turnover of intestinal epithelia in preclinical animal species and humans. Drug Metab. Dispos. 42, 2016–2022 (2014).

49. Flier, L. G. van der & Clevers, H. Stem Cells, Self-renewal, and differentiation in the intestinal epithelium. Annu. Rev. Physiol. 71, 241–260 (2009).

50. Rawat, P. S., Li, Y., Zhang, W., Meng, X. & Liu, W. Hungatella hathewayi, an efficient glycosaminoglycan-degrading Firmicutes from human gut and its Chondroitin ABC Exolyase with high activity and broad substrate specificity. Appl. Environ. Microbiol. 88, e01546-22 (2022).

51. Murch, S. H. et al. Disruption of sulphated glycosaminoglycans in intestinal inflammation. Lancet 341, 711–714 (1993).

52. Hussein, R. K., Mencio, C. P., Katagiri, Y., Brake, A. M. & Geller, H. M. Role of chondroitin sulfation following spinal cord injury. Front. Cell Neurosci. 14, 208 (2020).

53. Hong, T.-T., White, A. J. & Lucchesi, B. R. Dermatan disulfate (Intimatan) prevents complement-mediated myocardial injury in the human-plasma-perfused rabbit heart. Int. Immunopharmacol. 5, 381–391 (2005).

54. Dehghani, T. et al. Selectin-targeting glycosaminoglycan-peptide conjugate limits neutrophil-mediated cardiac reperfusion injury. Cardiovasc. Res. 118, 267–281 (2020).

55. Hori, Y. et al. Effects of chondroitin sulfate on colitis induced by dextran sulfate sodium in rats. Jpn. J. Pharmacol. 85, 155–160 (2001).

56. Turner, D. et al. Appraisal of the pediatric ulcerative colitis activity index (PUCAI). Inflamm. Bowel Dis. 15, 1218–1223 (2009).

57. Hyams, J. et al. Evaluation of the pediatric Crohn disease activity index: a prospective multicenter experience. J. Pediatr. Gastroenterol. Nutr. 41, 416–421 (2005).

58. Hamai, A. et al. Two distinct Chondroitin Sulfate ABC Lyases: an endoeliminase yielding tetrasaccharides and an exoeliminase preferentially acting on oligosaccharides. J Biol Chem 272, 9123–9130 (1997).

59. Prabhakar, V., Capila, I., Soundararajan, V., Raman, R. & Sasisekharan, R. Recombinant expression, purification, and biochemical characterization of Chondroitinase ABC II from Proteus vulgaris *. J Biol Chem 284, 974–982 (2009).
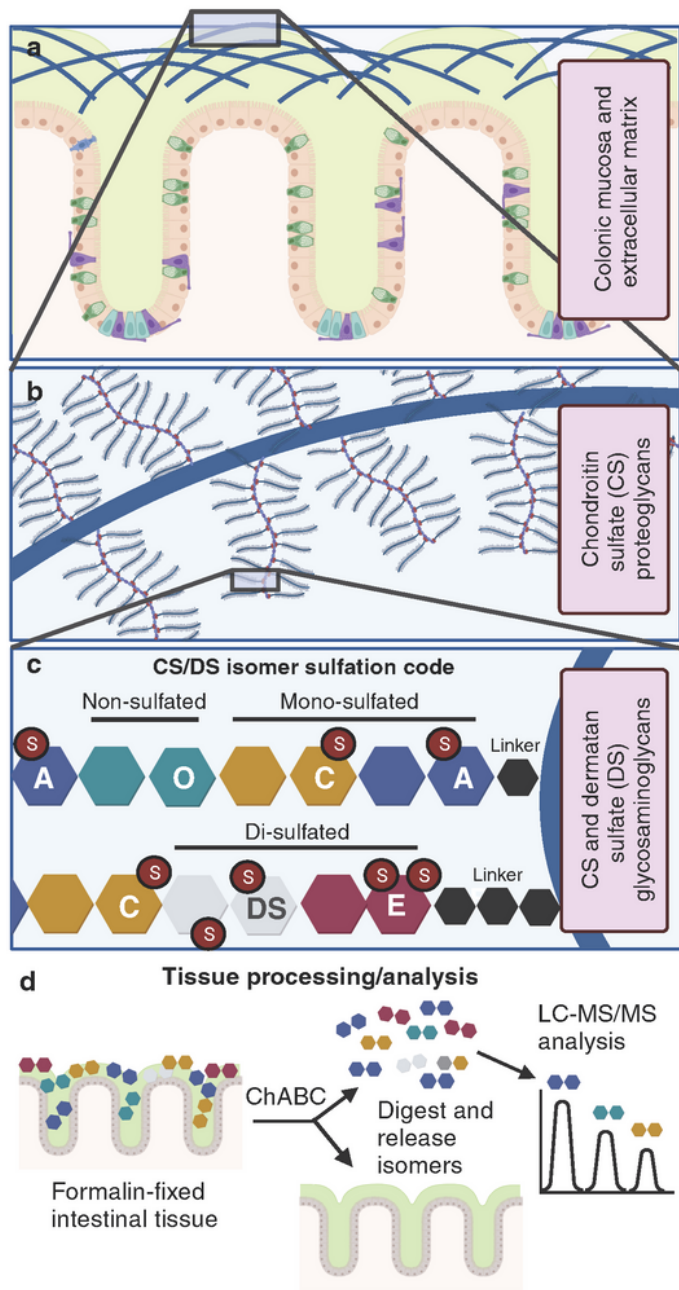
Figures

Figure 1

Chondroitin sulfate (CS) and dermatan sulfate (DS) glycosaminoglycan isomers and their relation to the intestinal extracellular matrix. Diagram of the (**a**) colonic intestinal extracellular matrix highlighting the (**b**) CS proteoglycan network and the (**c**) CS and DS glycosaminoglycan (CS/DS-GAG) chains, with the non-sulfated (CS-O or 0S), mono-sulfated (CS-C or 6S and CS-A or 4S), and di-sulfated (DS or 2S4S and CS-E or 4S6S) isomer units identified by the unique location of their sulfate group, which determines their

physiochemical properties. (**d**) Outline of tissue processing in which formalin-fixed and paraffin embedded intestinal biopsies taken during endoscopy are incubated with Chondroitinase ABC enzyme (ChABC) to digest all the CS/DS-GAG chains into individual isomer subunits, which are then collected, purified, and quantitatively analyzed by liquid chromatography tandem mass spectrometry (LC-MS/MS). Created with BioRender.com.
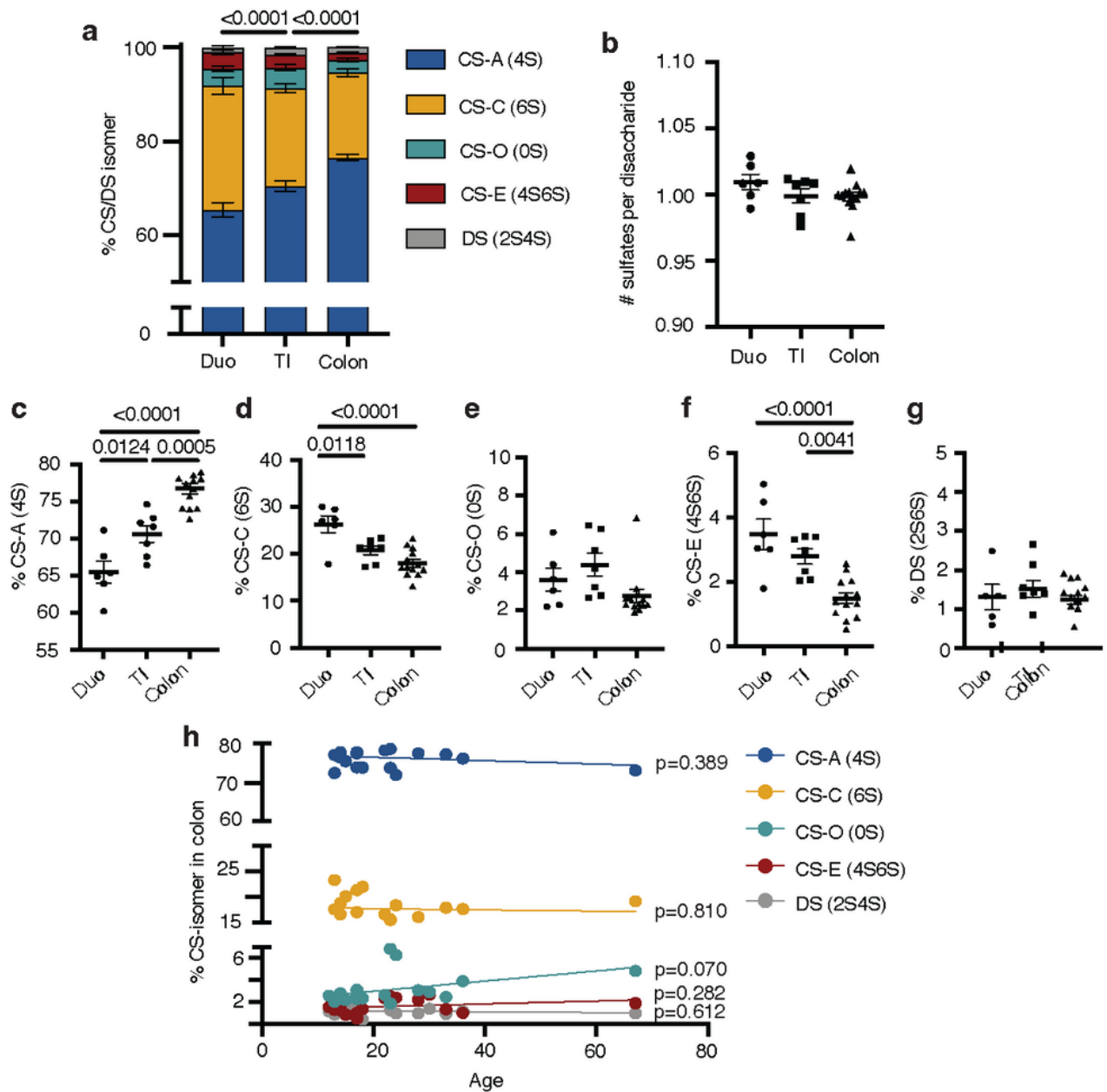

Figure 2

Chondroitin sulfate (CS) and dermatan sulfate (DS) isomer composition in normal bowel. (**a**) CS/DS isomer abundance in 13 pediatric patients without intestinal inflammation in intestinal biopsies from duodenum (duo, n=6), terminal ileum (TI, n=7), and colon tissue (n=13). (**b**) Sulfation patterns (i.e. average number of sulfate groups per individual disaccharide unit) in each location of bowel in pediatric patients. Isomer percentage compared in each area of bowel (duo, TI, and colon) for (**c**) CS-A, (**d**) CS-C, (**e**), CS-O, (**f**) CS-E, and (**g**) DS. (**h**) Colonic CS isomer abundance in the above 13 pediatric patients and 6 adult patients without intestinal inflammation plotted by age. P-values not listed in **b-g** are >0.05. Error bars represent SEM.
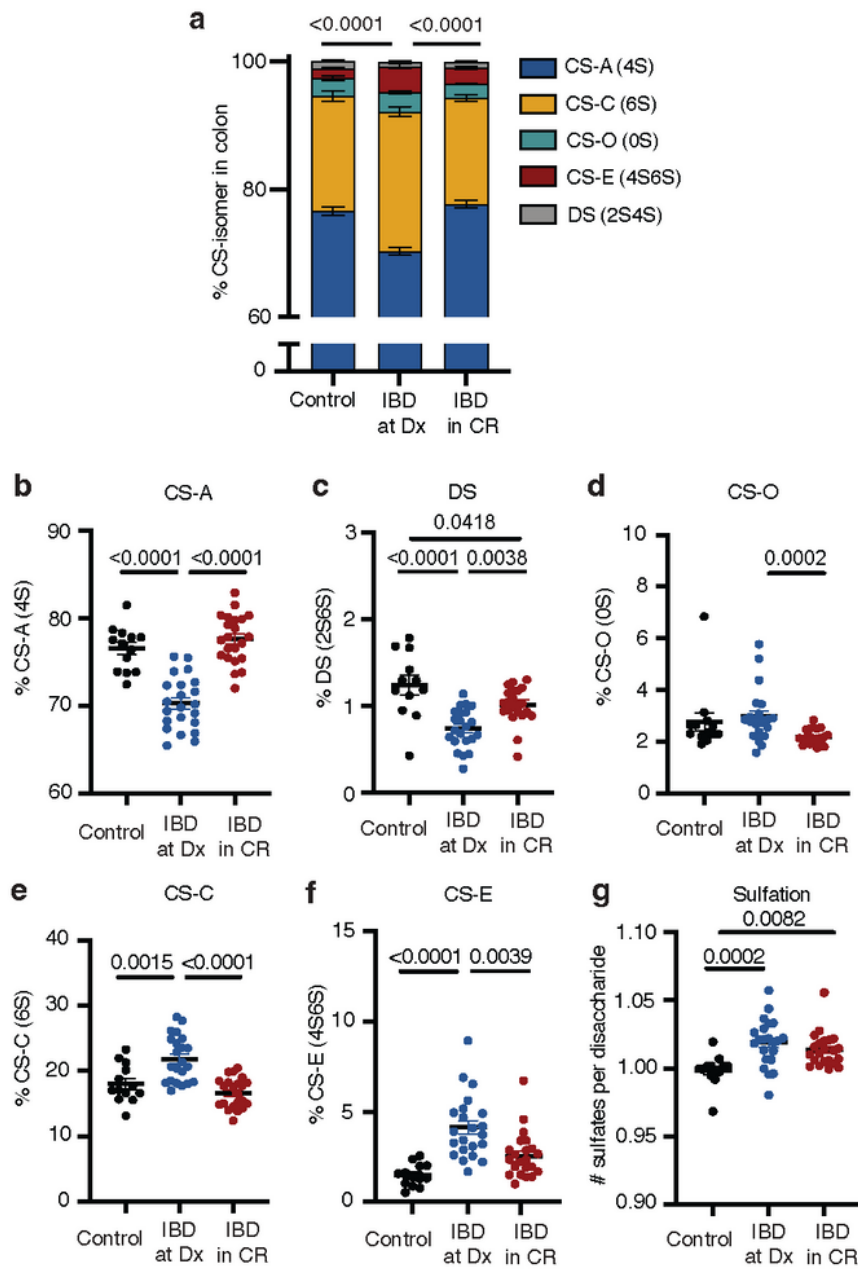
Figure 3

Chondroitin sulfate and dermatan sulfate (CS/DS) isomer profiles are altered in active IBD. (a) CS/DS isomer abundance in the colons of the same control patients in Figure **1a** (n=13) compared to individuals with IBD with colonic involvement (UC and CD colitis) at diagnosis with active clinical and histopathologic disease (IBD at Dx, n=22) and individuals with IBD with colonic involvement at diagnosis who were in clinical remission on IBD therapy when biopsies were acquired (IBD in CR, n=22). The relative

abundance of (**b**) CS-A and (**c**) DS is significantly lower in patients with active colonic IBD at Dx compared to control patients, which increases in patients with IBD in CR compared to IBD at Dx. (**d**) CS-O isomer abundance is not significantly altered by active IBD compared to controls, but decreases in patients in IBD in CR. (**e**) CS-C and (**f**) CS-E increase significantly in IBD at Dx compared to controls and decrease in IBD in CR compared to IBD at Dx. (**g**) Net sulfation per isomer is increased in IBD at Dx compared to controls patients and does not change significantly in IBD in CR compared to IBD at Dx, remaining significantly elevated compared to controls. P-values not listed in **b-g** are >0.05. Error bars represent SEM.
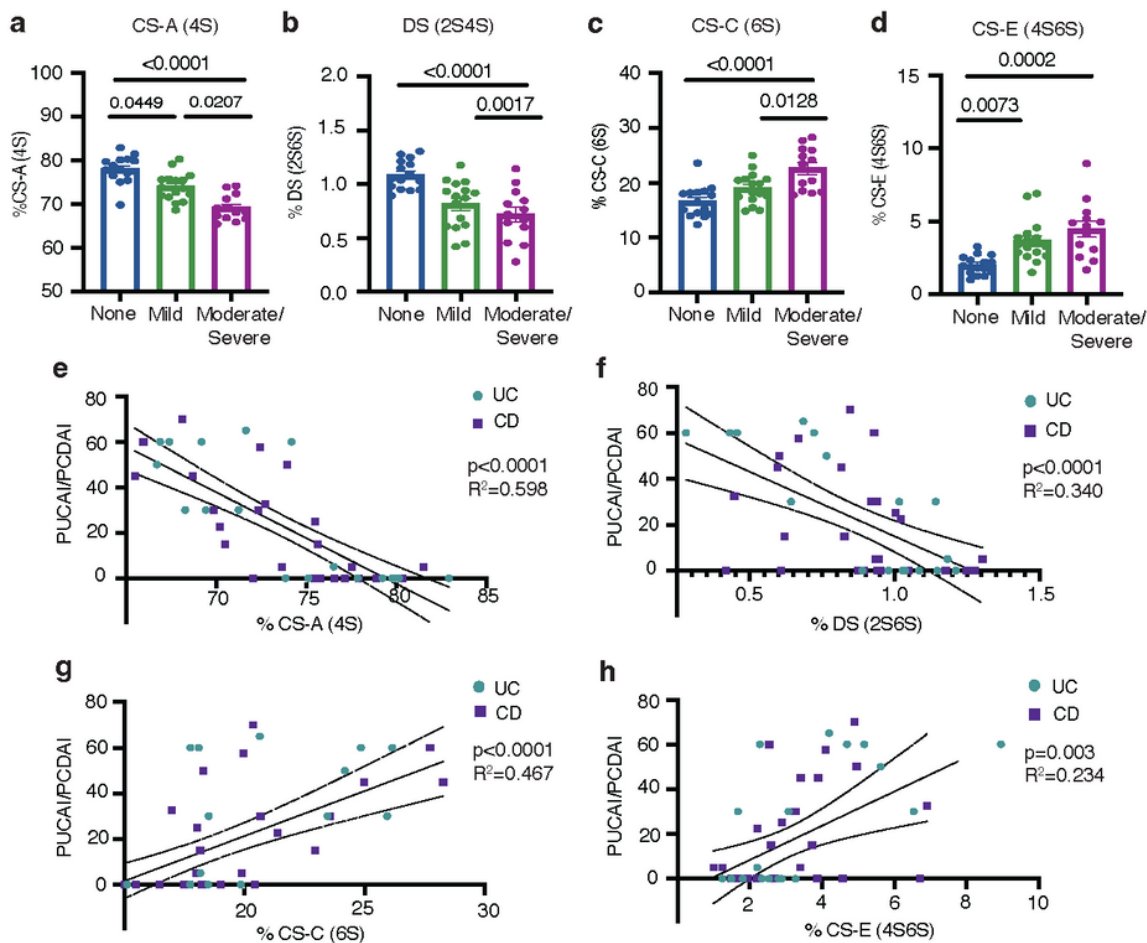

Figure 4

Figure 4

Chondroitin sulfate (CS) and dermatan sulfate (DS) isomer abundance correlates with histopathologic and clinical IBD activity. The abundance of pro-stabilizing isomers (**a**) CS-A and (**b**) DS in colonic tissue

from patients with and without IBD decreases in a stepwise fashion with the degree of pathologic inflammation, while the abundance of pro-inflammatory isomers (**c**) CS-C and (**d**) CS-E increases in a stepwise fashion in association with the degree of pathologic inflammation. Clinical IBD activity in patients with IBD with colonic involvement (UC and CD colitis), as measured by the Pediatric Ulcerative Colitis Activity Index and the Pediatric Crohn's Disease Activity Index (PUCAI and PCDAI) scores correlates inversely with the abundance of pro-stabilizing isomers (**e**) CS-A and (**f**) DS in the colon. Conversely, PUCAI/PCDAI scores increase in proportion to the abundance of pro-inflammatory isomers (**g**) CS-C and (**h**) CS-E. P-values not listed in **a-d** are >0.05. Error bars represent SEM.

Supplementary Files

This is a list of supplementary files associated with this preprint. Click to download.

- SupplementalFiguresScientificReports.pdf